Journal of Crystal Growth 334 (2011) 165–169

Contents lists available at ScienceDirect

Journal of Crystal Growth

journal homepage: www.elsevier.com/locate/jcrysgro

Growth and characterisation of Li_xCoO_2 single crystals

Loreynne Pinsard-Gaudart [a,b,*], Vasile-Cristian Ciomaga [a,b], Oana Dragos [a,b], Régis Guillot [a,b], Nita Dragoe [a,b]

[a] Univ. Paris-Sud, Institut de Chimie Moléculaire et des Matériaux d'Orsay, UMR8182, Bât 410, Orsay 91405, France
[b] CNRS, Orsay 91405, France

ARTICLE INFO

Article history:
Received 22 February 2011
Received in revised form
12 July 2011
Accepted 24 July 2011
Communicated by V. Fratello
Available online 29 July 2011

Keywords:
A1. de-intercalation
A2. Single crystal growth
B1. Lithium compounds

ABSTRACT

Centimetre-size single crystals of $LiCoO_2$ were successfully grown using a floating-zone method associated with an image furnace. A high-pressure oxygen atmosphere and a relatively small growth speed were found necessary to prevent the formation of impurity phases in the grown crystal. A single crystal with a reduced amount of lithium was obtained by means of the chemical de-lithiation process using as grown $LiCoO_2$ single crystal as the starting material. Growth conditions together with magnetic and structural properties of these crystals are discussed here.

1. Introduction

Alkaline layered cobalt oxides (A_xCoO_2) have been intensively studied because of their complex structural features [1], interesting physical properties, for instance metallic state [2], large thermoelectric power [3,4] or superconductivity for Na derivative [5], as well as their considerable technological significance as positive electrode material in lithium-ion batteries [6–11]. Recently it has been shown that this family of compounds could be used for non-volatile memory inscription implying ion-migration processes [12]. High temperature synthesised $LiCoO_2$ adopts a layered rock salt structure with trigonal symmetry, and spacegroup R -3 m, consisting of CoO_2 layers of face sharing octahedra [8,13]. The lithium atoms are located at the octahedral sites between the CoO_2 layers. After delithiation, lithium-deficient compounds Li_xCoO_2 can be obtained [14–16]; this phase belongs to the same space group. It has also been found that the end member of these compounds, CoO_2, can be obtained by electrochemical de-intercalation [17–19]. An extensive review of the synthesis methods, defects and physical properties of Li_xCoO_2 was published by Antolini [20].

Magnetic measurements indicate that, for stoichiometric $LiCoO_2$, Co^{3+} ions are in a low spin configuration and no magnetic transition was observed. On the other hand, for nonstoichiometric compounds ($x<1$), the magnetic measurements show a magnetic transition below 175 K [21,22].

Small $LiCoO_2$ single crystals have been previously obtained using the flux technique [23,24]. Studies of the anisotropic properties of these compounds require sizeable single crystals and this led us to investigate the growth of larger dimension crystals. In this work, we present the floating zone (FZ) method for growing $LiCoO_2$ single crystals as well as their structures and properties.

2. Experimental procedure

Single-phase polycrystalline samples of $LiCoO_2$ were prepared by the standard solid-state reaction route using commercially available Li_2CO_3 and Co_3O_4 (Alfa Aesar, 99.7% purity) powders. Stoichiometric amounts of the starting powders were mixed and calcined at 950 °C for 16 h in air. The samples were re-ground and mixed with additional Li_2CO_3 (Table 1), which was added to compensate for the expected evaporation of lithium in the single crystal growth procedure. The feed material for the single crystal growth process was prepared in the form of cylindrical rods, of about 6 mm in diameter and 7 cm in length, by isostatically compressing the powder under 2500 bar. The rods were subsequently sintered at 1050 °C for 16 h in air. The single crystal growth experiments were carried out using the FZ technique in an optical image furnace (Crystal System Inc., Japan) equipped with four 300 W halogen lamps, under a high pressure of oxygen (Table 1).

Several different techniques were used to characterise the grown single crystal of $LiCoO_2$ and single crystals obtained after Li de-intercalation. Powder X-ray diffraction was done on a Philips PW 3710 diffractometer for checking the phase purity. The orientation of

* Corresponding author at: Univ. Paris-Sud, Institut de Chimie Moléculaire et des Matériaux d'Orsay, UMR8182, Bât 410, Orsay 91405, France.
E-mail address: loreynne.pinsard-gaudart@u-psud.fr (L. Pinsard-Gaudart).

0022-0248/$ - see front matter © 2011 Elsevier B.V. All rights reserved.
doi:10.1016/j.jcrysgro.2011.07.024

Table 1
Example conditions used to prepare single crystal sample of $LiCoO_2$.

Material	Lithium excess (%)	Atmosphere (atm/O_2)	Growth rate (mm/h)
$LiCoO_2$	0	9	–
$LiCoO_2$	10	9	–
$LiCoO_2$	20	9	–
$LiCoO_2$	50	7	2
$LiCoO_2$	75	7	2
$LiCoO_2$	100	8–9	2
$LiCoO_2$	100	8–9	5
$LiCoO_2$	100	8–9	5 and 3

the grown crystals was determined by the Laüe back reflection diffraction technique. The structure determination was carried on a Kappa APPEX II Bruker single crystal X-ray diffractometer using monochromatised Mo Kα radiation (λ=0.71073 Å). The data were corrected for Lorentz, polarisation and absorption effects. The structures were solved by direct methods using SHELXS-97 and refined against F^2 by full-matrix least-square techniques using SHELXL-97 [25] with anisotropic displacement parameters for all atoms. All calculations were performed using the crystallographic software package WINGX [26]. The magnetisation studies of the $LiCoO_2$ and $Li_{0.63}CoO_2$ single crystals were carried out as a function of temperature and applied field using a SQUID magnetometer (Quantum Design). Seebeck coefficients were measured using a DC differential technique, obtained with gradients up to 0.2 K/min, in a laboratory made closed cycle cryostat system from about 30 K to 300 K. AC and DC resistivities were measured on thin crystal platelets, in *ab* plane, from 77 K to 400 K using a four probes method by applying AC (measurement at 71 Hz) or DC currents from 50 to 250 nA using an SRS830 lock-in amplifier or a Keithley 2182 nanovoltmeter, respectively.

3. Results and discussion

In order to obtain centimetre-size single crystals of $LiCoO_2$, we optimised the growth parameters (atmosphere, pressure, growth speed and the feed rod composition) in the image furnace. Several single crystal growth experiments, under different conditions, were carried out. In Table 1, we present relevant experiments for different values of the O_2 pressure, the growth speed and the composition of the feed rod. Preliminary experiments, the first line in Table 1, indicated that an excess of lithium was required (strong evaporation during fusion and instability of the molten zone). For the subsequent growth experiments the feed rods had 10%–20% excess of lithium. Even in these cases the molten zone could not be stabilised, probably because the lithium excess was not sufficient. In the following experiments we used feed rods prepared with up to 100% lithium excess and growth speeds of 2–5 mm/h, under a pressure of about 8–9 atm of oxygen. Higher speed seems to be more adapted for the stabilisation of the molten zone in these conditions. The best results were obtained by starting with a growth speed of 5 mm/h, and after the molten zone was stabilised the growth speed was reduced to 3 mm/h. The resulting crystals had typically 10 cm length but only about 2 cm length of the as grown crystal is of single phase with hexagonal structure and no impurities or inclusions. Fig. 1 shows a 2 cm length of the crystal cut from the as grown crystal ingot. Electron microscopy images of sections cut at the end of the crystal do not show the presence of secondary phases. Crystals are black and cleave very easily perpendicular to the [0 0 1] direction, which is perpendicular to the growth direction. This is the same direction growth as the one observed for Na_xCoO_2 crystals [27]. We could obtain cleaved pieces of single crystals of $20 \times 4 \times 3$ mm^3.

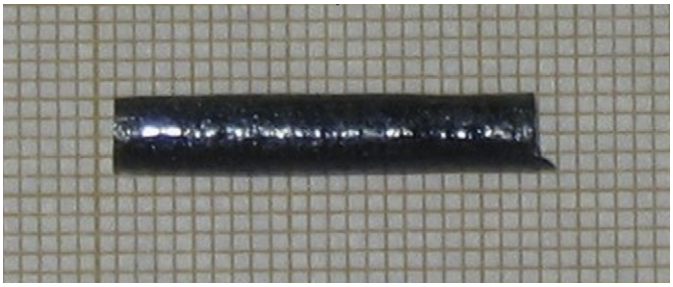

Fig. 1. A piece of an as grown single crystal of $LiCoO_2$.

Table 2
Structural parameters for Li_xCoO_2 (x=1 and 0.63). Space group R –3 m. Atomic positions: Co: 3b (0 0 0.5); Li: 3a (0 0 0); O: 6c (0 0 z).

Formula	$LiCoO_2$	$Li_{0.63}CoO_2$
Fw	97.87	95.16
a [Å]	2.81280(10)	2.80760(10)
c [Å]	14.0272(9)	14.2129(8)
V [Å^3]	96.112(8)	97.025(7)
λ [Å]	0.71075	0.71075
T [K]	280	280
Z	3	3
Crystal size mm^3	$0.316 \times 0.276 \times 0.153$	$0.800 \times 0.340 \times 0.140$
ρ_{calcd} [g cm^{-3}]	5.073	4.886
μ(Mo$_K\alpha$) [mm^{-1}]	12.727	12.603
θ range [deg., min.–max.]	4.36–47.26	4.30–48.00
No. of data collected	1448	1378
No. of unique data	140	133
R (int)	0.0325	0.1164
No. of variable parameters	9	10
No. of obs. refl.[a]	140	132
R obs., all[b]	0.0511	0.0493
R_w obs., all[c]	0.1276	0.1238
S	1.031	1.177
$(\Delta/\sigma)_{max}$	0.000	0.001
x (occupation of Li)	1	0.61(16)
z (position of O (0 0 z)	0.7604(3)	0.7630(3)

[a] Data with $F_o > 4\sigma(F_o)$.
[b] $R=\sum||F_o|-|F_c||/\sum|F_o|$.
[c] $R_w=[\sum w(|F_o^2|-|F_c^2|)^2/\sum w|F_o^2|^2]^{1/2}$.

After successful single-crystal growth of $LiCoO_2$, several single crystals with lower concentrations of lithium were obtained by chemical de-intercalation of lithium ions by mixing pristine $LiCoO_2$ single-crystals with excess Br_2 (Li:Br 40 times in molar ratio) dissolved in dry acetonitrile. After 7 days of stirring, the obtained sample was washed with acetonitrile several times and stored in a dessicator.

Single-crystal X-ray diffraction measurements were performed on thin specimens obtained by cleaving the as grown crystal as well as the de-intercalated one. The temperature of the crystal during data acquisition was maintained at 280 K under dry nitrogen atmosphere in order to prevent the degradation of the cleaved surface. Structural parameters for the two single crystals ($LiCoO_2$ and $Li_{0.63}CoO_2$), determined by the least-square refinement, are given in Table 2. After the lithium de-intercalation the crystal structure remained hexagonal as for the parent $LiCoO_2$ crystal; this structure is presented in Fig. 2. Lattice parameters are slightly smaller than those found for powder samples of similar compositions [13,15] but in very good agreement with previous data on single crystals [16]. The c parameter value increases with reduction in the lithium quantity in $Li_{0.63}CoO_2$ while the lattice

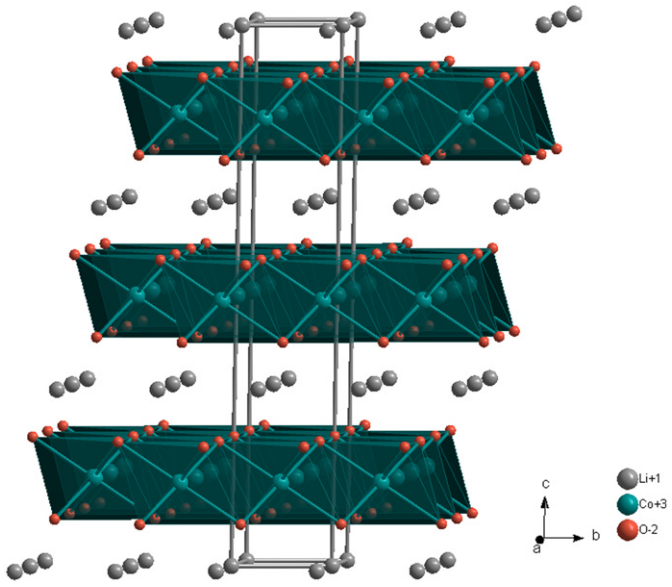

Fig. 2. Crystal structure of $LiCoO_2$.

parameter *a* shows an opposite variation. This is consistent with the removal of lithium from $LiCoO_2$, which leads to an increase of the spacing between layers due to repulsive forces between negatively charged oxygen ions. This, in consequence, results in expansion of the structure in the direction parallel to the *c*-axis [28]. The observed slight decrease in the *a* lattice parameter can be explained by the oxidation of the Co^{3+} ions and formation of smaller Co^{4+} ions.

Magnetisation measurements on the crystals were done in two orientations relative to the applied field: (i) perpendicular to the *c*-axis and (ii) parallel to the c-axis. The temperature dependence for the two directions for the $LiCoO_2$ and $Li_{0,63}CoO_2$ single crystals under an applied field of 1000 Oe is shown in Fig. 3.

The magnetisation measurements are very sensitive to the presence of magnetic impurities like Co_3O_4 and CoO, which exhibit anti-ferromagnetic transitions at 40 K and 290 K, respectively. No such magnetic transition was observed in these samples. For the two single crystals the magnetisation curves as functions of temperature showed a Curie–Weiss behaviour, independent of the orientation relative to the magnetic field. For both samples the measurements with the field in *ab*-plane showed a slight anomaly at around 170 K, see the inset in Fig. 3, similar to the one observed previously at 175 K in polycrystalline $LiCoO_2$ [29]. A deviation from the Curie–Weiss behaviour was found below 50 K, which may be due to the impurities or due to the magnetic correlations manifesting below this temperature. The χ_0, μ_{eff} and Θ_{CW} obtained from a Curie–Weiss fit with and without a temperature independent term (χ_0) of the χ data, fitted in the temperature range 150 K–300 K, are shown in Table 3.

The experimental magnetic moments for both crystals are slightly higher than the expected values (0 and 1.22 for the two compositions, respectively). The fit considering temperature independent paramagnetism gave values closer, but a little larger, than the expected values, particularly for an $S=0$ stoichiometric $LiCoO_2$ compound. A very small decrease of the stoichiometry may explain the increase of the effective moment [30]. It has been shown recently that the "real" stoichiometry of the Li sample might be difficult to control [31]. Another possible origin of this magnetic behaviour is a charge disproportion of Co^{3+} ions into Co^{2+} and Co^{4+} ions [30] or the existence of defects or unusual spin state of the cobalt ions as in the case of layered cobaltate Na_xCoO_2 [28]. A recent report indicated that additional defects

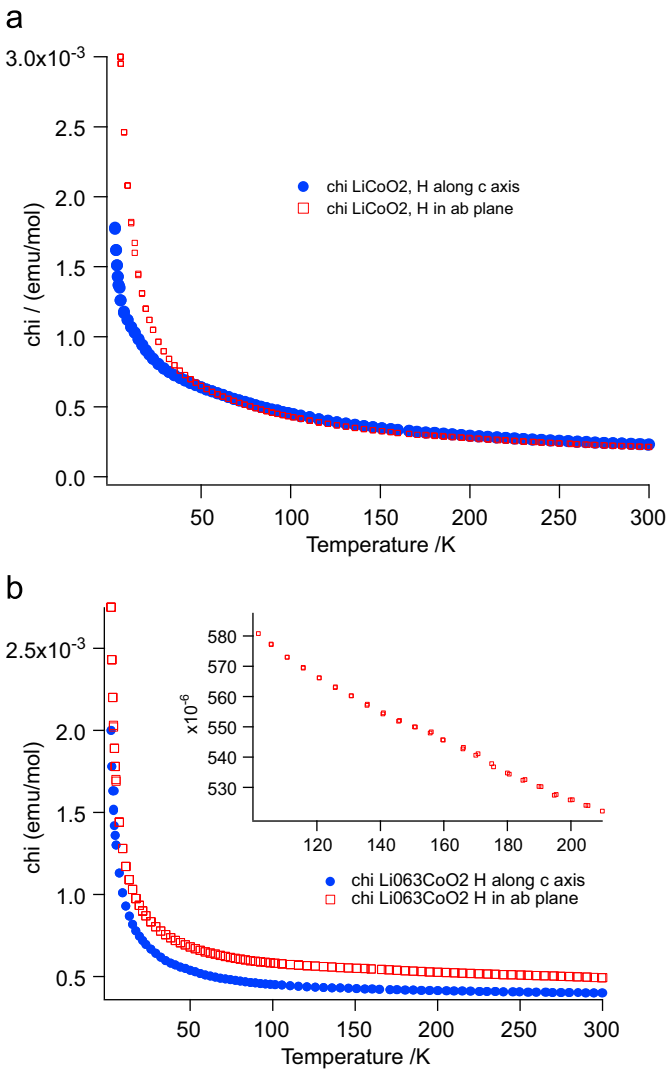

Fig. 3. Temperature dependence of DC magnetisation in the ab-plane and along the c-axis for $LiCoO_2$ (a) and $Li_{0.63}CoO_2$ (b) single crystals samples under an applied field of 1000 Oe.

Table 3
Magnetic parameters for Li_xCoO_2 crystals, with applied field parallel and perpendicular to the c-axis, fitted with and without a TIP parameter fit.

	χ_0 ($\times 10^6$)		Θ_{CW} (K)		$\mu_{eff\ exp}$ (μ_B)	
	$H\|(ab)$	$H\|c$	$H\|(ab)$	$H\|c$	$H\|(ab)$	$H\|c$
$LiCoO_2$	–	–	−131(2)	−146(2)	0.84	0.90
$Li_{0.63}CoO_2$	–	–	−1167(14)	−2184(15)	2.36	2.77
$LiCoO_2$	25(1)	4.2(2)	−35(3)	−53(4)	0.29	0.51
$Li_{0.63}CoO_2$	62(6)	79(4)	−854(0)	−1315(0)	1.39	1.35

and impurities are possible, not all of which are detectable by laboratory X-ray diffraction, in "stoichiometric" $LiCoO_2$ [32].

A study of the magnetisation behaviour as a function of the applied magnetic field was carried out at several temperatures (2, 30 and 50 K) and in an interval of applied magnetic field −5.5 T to +5.5 T. At high temperatures (30 K and 50 K) the magnetic behaviour of the two samples is linear with the field, which is typical of paramagnetic materials. At low temperatures (2 K) a departure from the linearity is observed, which indicates the presence of short-range ferromagnetic (or ferrimagnetic) interactions (Fig. 4). The magnetisation behaviour in the single crystals

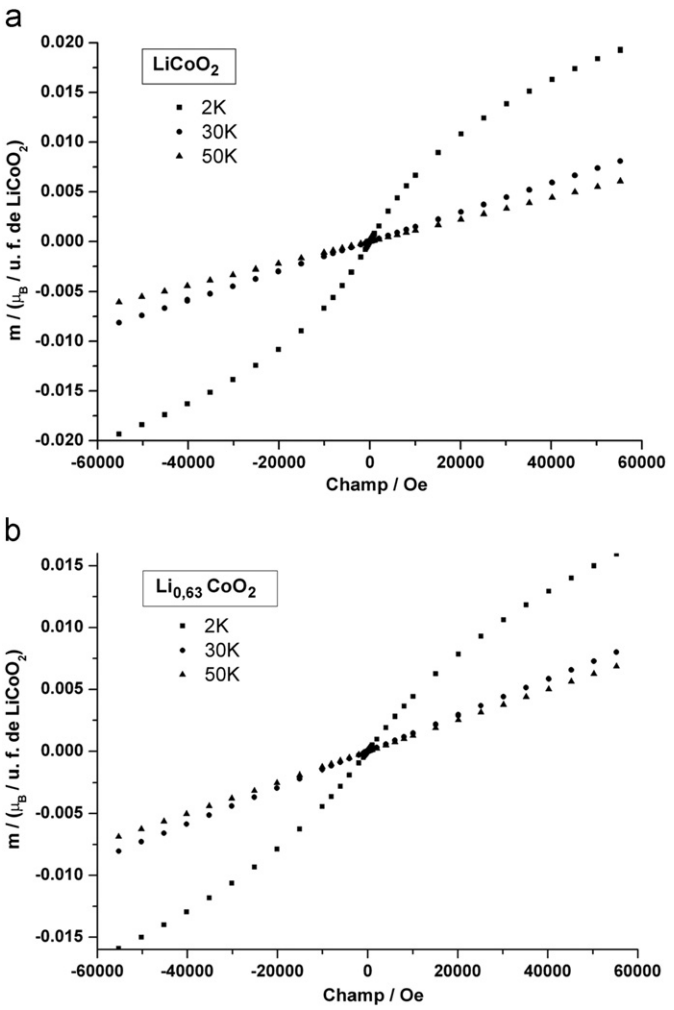

Fig. 4. DC magnetisation loop curves versus magnetic field for (a) $LiCoO_2$ and (b) $Li_{0.63}CoO_2$ single-crystals.

of Li_xCoO_2 under applied magnetic field is rather complex, similar to that of Na_xCoO_2 compounds [28,32,33].

Previously, the electrical resistivity was measured on a small crystal grown by a flux method and an anisotropy of about 500 at 300 K was found [34]. We could not measure the resistivity of these samples perpendicular to the *ab*-plane, probably because of the fact that the crystal cleaves easily and sudden "jumps" in the resistivity values are observed. This is also the case for other layered materials; see for instance the case of Na_xCoO_2 in Fig. 4 of Ref. [27]. Resistivity in the *ab*-plane was measured by placing four contacts on a platelet, whose thickness was estimated at about 10 μm (or even less if there are no contacts between several plates). As such resistivity is estimated just based on this geometrical factor, but the trend is indicative of a semiconductor. This curve is shown in the inset of Fig. 5. This result is close to the previous experiments on powders of the same compositions [15],where transport is thermally activated with a variation of the activation energy with temperature.

For the as grown crystal, two pieces of a same crystal were cut and the Seebeck coefficients' functions versus temperature were measured (Fig. 5). We observed a small difference between the measurements perpendicular and parallel to the c-axis. We note a feature appearing at about 160 K in the thermoelectric power for the sample measured in the *ab* plane that might be related to the one observed in the magnetic data shown in Fig. 3 and at 180 K for the resistivity data shown in the inset of Fig. 5. These

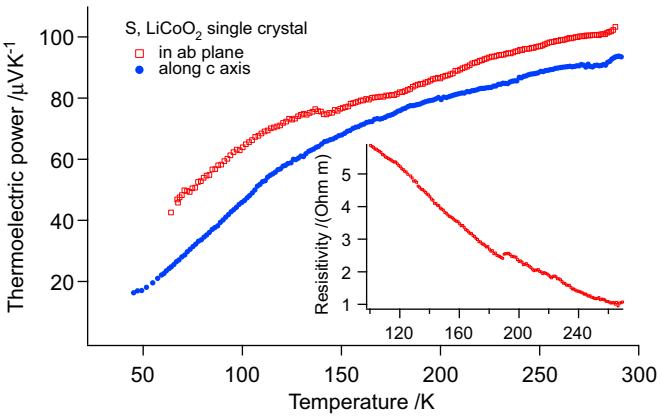

Fig. 5. Seebeck coefficient of $LiCoO_2$ single crystals along and perpendicular to the c axis; inset: AC resistivity of thin platelets of $LiCoO_2$ in the *ab*-plane.

"features" are of unknown origin but might be related with slipping of *ab*-planes during the measurement.

The values of the measured Seebeck coefficient, around 100 μV/K at 300 K, are comparable with the value reported in the literature for powders [15] or for the thin film samples of Li_xCoO_2, whose thermoelectric factor increases with the lithium content [35]. These values are consistent with the existence of non-metallic state for high lithium content samples associated with large thermoelectric factors and rather large resistivities (of the order of Ω m) contrary to the case of sodium-rich Na_xCoO_2, where metallic-like states and large thermopower are coexistent either because of spin entropy [36], electron correlations [37] or a narrow band model [38]. We could not measure the transport properties of de-intercalated crystals, which were too brittle.

4. Conclusions

Centimetre- size single crystals of $LiCoO_2$ were grown with a floating zone image furnace. Lithium deficient singles crystals were obtained by chemical de-intercalation. The single crystal X-ray diffraction study confirmed the trigonal R -3 m space group for both single crystals. The magnetic measurements as a function of temperature show a Curie–Weiss behaviour for the two single crystals and the value of the magnetic moment was found bigger than the expected value. A weak ferromagnetic or ferrimagnetic behaviour was found at low temperature, which indicates the presence of short-range interactions. Anisotropic thermoelectric power coefficients were determined.

Acknowledgement

This work was supported by the Triangle de la Physique, contract "SYMTCOB" no.2008-054T.

References

[1] R. Berthelot, D. Carlier, C. Delmas, Nature Materials 10 (2011) 74.
[2] T. Tanaka, S. Nakamura, S. Iida, Japanese Journal of Applied Physics Part 2-Letters 33 (1994) L581.
[3] I. Terasaki, Y. Sasago, K. Uchinokura, Physical Review B 56 (1997) 12685.
[4] W. Koshibae, K. Tsutsui, S. Maekawa, Physical Review B 62 (2000) 6869.
[5] R.E. Schaak, T. Klimczuk, M.L. Foo, R.J. Cava, Nature 424 (2003) 527.
[6] M. Menetrier, A. Levasseur, C. Delmas, J.F. Audebert, P. Hagenmuller, Solid State Ionics 14 (1984) 257.
[7] M. Menetrier, A. Levasseur, C. Delmas, Materials Science and Engineering B—Solid State Materials for Advanced Technology 3 (1989) 103.
[8] T. Ohzuku, A. Ueda, M. Nagayama, Y. Iwakoshi, H. Komori, Electrochimica Acta 38 (1993) 1159.

[9] K. Sekai, H. Azuma, A. Omaru, S. Fujita, H. Imoto, T. Endo, K. Yamaura, Y. Nishi, S. Mashiko, M. Yokogawa, Journal of Power Sources 43 (1993) 241.
[10] J. Molenda, C. Delmas, P. Hagenmuller, Solid State Ionics 9-10 (1983) 431.
[11] C. Delmas, M. Menetrier, L. Croguennec, S. Levasseur, J.P. Peres, C. Pouillerie, G. Prado, L. Fournes, F. Weill, International Journal of Inorganic Materials 1 (1999) 11.
[12] O. Schneegans, A. Moradpour, O. Dragos, S. Franger, N. Dragoe, L. Pinsard-Gaudart, P. Chretien, A. Revcolevschi, Journal of the American Chemical Society 129 (2007) 7482.
[13] H.J. Orman, P.J. Wiseman, Acta Crystallographica Section C—Crystal Structure Communications 40 (1984) 12.
[14] R. Gupta, A. Manthiram, Journal of Solid State Chemistry 121 (1996) 483.
[15] S. Levasseur, M. Menetrier, E. Suard, C. Delmas, Solid State Ionics 128 (2000) 11.
[16] Y. Takahashi, N. Kijima, K. Dokko, M. Nishizawa, I. Uchida, J. Akimoto, Journal of Solid State Chemistry 180 (2007) 313.
[17] C. De Vaulx, M.H. Julien, C. Berthier, S. Hebert, V. Pralong, A. Maignan, Physical Review Letters 98 (2007).
[18] T. Motohashi, Y. Katsumata, T. Ono, R. Kanno, M. Karppinen, H. Yamauchi, Chemistry of Materials 19 (2007) 5063.
[19] T. Motohashi, T. Ono, Y. Katsumata, R. Kanno, M. Karppinen, H. Yamauchi, Journal of Applied Physics 103 (2008).
[20] E. Antolini, Solid State Ionics 170 (2004) 159.
[21] J. Sugiyama, H. Nozaki, J.H. Brewer, E.J. Ansaldo, G.D. Morris, C. Delmas, Physica B—Condensed Matter 374 (2006) 148.
[22] A. Ito, K. Tanaka, H. Kawaji, T. Atake, N. Ando, Y. Hato, Journal of Thermal Analysis and Calorimetry 92 (2008) 399.
[23] J. Akimoto, Y. Gotoh, Y. Oosawa, Journal of Solid State Chemistry 141 (1998) 298.
[24] J. Akimoto, Y. Gotoh, Molecular Crystals and Liquid Crystals 341 (2000) 947.
[25] G.M. Sheldrick, Shelxl 97 Program, 1997.
[26] L.J. Farrugia, Journal of Applied Crystallography 32 (1999) 837.
[27] D.P. Chen, H.C. Chen, A. Maljuk, A. Kulakov, H. Zhang, P. Lemmens, C.T. Lin, Physical Review B 70 (2004).
[28] T. Motohashi, R. Ueda, E. Naujalis, T. Tojo, I. Terasaki, T. Atake, M. Karppinen, H. Yamauchi, Physical Review B 67 (2003).
[29] J.T. Hertz, Q. Huang, T. McQueen, T. Klimczuk, J.W.G. Bos, L. Viciu, R.J. Cava, Physical Review B 77 (2008).
[30] J. Sugiyama, H. Nozaki, J.H. Brewer, E.J. Ansaldo, G.D. Morris, C. Delmas, Physical Review B 72 (2005).
[31] M. Menetrier, D. Carlier, M. Blangero, C. Delmas, Electrochemical and Solid State Letters 11 (2008) A179.
[32] A. Artemenko, M. Menetrier, M. Pollet, C. Delmas, Journal of Applied Physics 106 (2009).
[33] T. Motohashi, T. Ono, Y. Sugimoto, Y. Masubuchi, S. Kikkawa, R. Kanno, M. Karppinen, H. Yamauchi, Physical Review B 80 (2009).
[34] Y. Takahashi, Y. Gotoh, J. Akimoto, S. Mizuta, K. Tokiwa, T. Watanabe, Journal of Solid State Chemistry 164 (2002) 1.
[35] Y. Ishida, A. Mizutani, K. Sugiura, H. Ohta, K. Koumoto, Physical Review B 82 (2010).
[36] Y.Y. Wang, N.S. Rogado, R.J. Cava, N.P. Ong, Nature 423 (2003) 425.
[37] J.O. Haerter, M.R. Peterson, B.S. Shastry, Physical Review Letters 97 (2006).
[38] N. Kaurav, K.K. Wu, Y.K. Kuo, G.J. Shu, F.C. Chou, Physical Review B 79 (2009) 075105.